NASA TECHNICAL NOTE

NASA TN D-7165

NASA TN D-7165

HYDROGEN AND HYDROCARBON DIFFUSION FLAMES IN A WEIGHTLESS ENVIRONMENT

by John B. Haggard, Jr., and Thomas H. Cochran

Lewis Research Center

Cleveland, Ohio 44135

NATIONAL AERONAUTICS AND SPACE ADMINISTRATION • WASHINGTON, D. C. • FEBRUARY 1973

1. Report No.	2. Government Accession No.	3. Recipient's Catalog No.
NASA TN D-7165		

4. Title and Subtitle	5. Report Date
HYDROGEN AND HYDROCARBON DIFFUSION FLAMES IN A WEIGHTLESS ENVIRONMENT	February 1973
	6. Performing Organization Code

7. Author(s)	8. Performing Organization Report No.
John B. Haggard, Jr., and Thomas H. Cochran	E-6687
	10. Work Unit No. 502-28

9. Performing Organization Name and Address	11. Contract or Grant No.
Lewis Research Center National Aeronautics and Space Administration Cleveland, Ohio 44135	

12. Sponsoring Agency Name and Address	13. Type of Report and Period Covered
National Aeronautics and Space Administration Washington, D.C. 20546	Technical Note
	14. Sponsoring Agency Code

15. Supplementary Notes

Technical Film Supplement C-277 available on request.

16. Abstract

An experimental investigation was performed on laminar hydrogen-, ethylene-, and propylene-air diffusion flames burning in a weightless environment. The flames burned on nozzles with radii ranging from 0.051 to 0.186 cm with fuel Reynolds numbers at the nozzle exit from 9 to 410. Steady-state diffusion flames existed in a weightless environment for all the fuels tested. A correlation was obtained for their axial length as a function of Schmidt number, Reynolds number, and stoichiometric mole fraction. The maximum flame radii were correlated with the ratio of nozzle radius to average fuel velocity. The flames of ethylene and propylene on nozzles with radii 0.113 cm or larger appeared to be constantly changing color and/or length throughout the test. No extinguishment was observed for any of the gases tested within the 2.2 seconds of weightlessness.

17. Key Words (Suggested by Author(s))	18. Distribution Statement
Diffusion flames Zero gravity Spacecraft safety	Unclassified - unlimited

19. Security Classif. (of this report)	20. Security Classif. (of this page)	21. No. of Pages	22. Price*
Unclassified	Unclassified	29	$3.00

* For sale by the National Technical Information Service, Springfield, Virginia 22151

HYDROGEN AND HYDROCARBON DIFFUSION FLAMES IN A WEIGHTLESS ENVIRONMENT

by John B. Haggard, Jr., and Thomas H. Cochran

Lewis Research Center

SUMMARY

An experimental investigation was performed on laminar hydrogen-, ethylene-, and propylene-air diffusion flames burning in a weightless environment. The flames burned on nozzles with radii ranging from 0.051 to 0.186 centimeter with fuel Reynolds numbers at the nozzle exit from 9 to 410. Steady-state diffusion flames existed in a weightless environment for all the fuels tested. Their axial length was proportional to the product of the nozzle radius, the fuel Reynolds number, the one-half power of the Schmidt number, and a parameter that depends on the stoichiometric mole fraction. The maximum width of the steady-state flames was proportional to the nozzle radius and to the logarithm of the ratio of the nozzle radius to the average fuel velocity at the nozzle exit. The ethylene and propylene flames on nozzles with radii 0.113 centimeter or larger appeared to be constantly changing color and/or length throughout the test. No extinguishment was observed for any of the gases tested within the 2.2 seconds of weightlessness.

INTRODUCTION

In the past several years the Lewis Research Center has been conducting fire safety investigations on solids and gases burning in a weightless environment. Because of the lack of buoyancy in such an environment, the phenomena of burning is altered from the usual combustion processes occurring here on Earth. Therefore, a continuing effort has been made to examine the effect of gravity on flames burning in typical spacecraft environments.

Zero-gravity combustion studies relating to solids include the work of Andracchio and Aydelott (ref. 1), who measured the surface flame spread rate on thin plastic and paper slabs in an oxygen environment. Their results showed that the spread rate was

lower in zero gravity than in normal-gravity. Tests were also conducted by Cochran et. al. (ref. 2) in which Teflon coated wires were burned in supercritical oxygen. This work was in support of the investigation of the explosion on board the Apollo 13 vehicle.

Gaseous diffusion flames are another combustion process that can be affected by gravity. Cochran and Masica (ref. 3) investigated methane-air diffusion flames on circular nozzles and found that flames on nozzles 0.186 centimeter or larger extinguished in drop tower tests. Cochran and Masica (ref. 4) then made a preliminary survey of methane-air diffusion flames on relatively small radii nozzles (from 0.051 to 0.113 cm) and found that at high flow rates these flames were in steady state when in a weightlessness condition. Subsequently, Cochran (ref. 5) performed a detailed series of experiments with methane-air diffusion flames and found that the steady-state zero-gravity flame length was proportional to the fuel volumetric flow rate. In addition to the steady state and extinguished flames, transient flames (changing color and/or length throughout the test) were observed for certain flow conditions. It was concluded that there may not have been sufficient test time for the transient flames to come to steady state.

The purpose of the study reported herein is to extend the zero-gravity experimentation of gas jet diffusion flames burning in air to fuels other than methane in order to obtain general correlations for axial flame length and width and to examine flame existence in weightlessness. The experiments were conducted in a 2.2-second drop tower facility using ethylene, propylene, and hydrogen fuel gases. Nozzle radii ranged from 0.051 to 0.186 centimeter with the fuel Reynolds numbers at the nozzle exit ranging from 9 to 410.

In all of the work previously cited, as well as the current data, visual observations of high-speed motion picture film of the tests played a key role in analyzing the phenomena. Technical Film C-277, which summarizes all the work performed at the Lewis Research Center on solid and gas combustion in a weightless condition, is available upon request. A request card and a description of the film are included at the back of this report.

SYMBOLS

A constant

B constant

c_F fuel mole fraction in reaction zone

c_L fuel mole fraction at lower limit of flammability with air

c_U fuel mole fraction at upper limit of flammability with air

c_S fuel mole fraction at stoichiometric mixture

D	diffusion coefficient of fuel into air, cm^2/sec
$\bar{g}$	gravity level, ratio of system acceleration to earth's gravity
L	axial flame length, cm
L_s	axial length of steady-state flame in zero gravity, cm
L_1	average axial length of normal-gravity flame, cm
Q	flow rate of fuel nozzle exit under standard conditions, cm^3/sec
R_0	inside nozzle radius, cm
R_M	maximum flame radius, cm
R_{M1}	maximum flame radius in normal gravity, cm
R_{M0}	maximum flame radius in zero gravity, cm
Re	Reynolds number of fuel at nozzle exit, $\bar{V}R_{0/\nu}$
Sc	Schmidt number of fuel at nozzle exit, ν/D
$\bar{V}$	average axial velocity, cm/sec
ν	kinematic viscosity, cm^2/sec
τ_F	fuel time, $(R_0)(10^3)/(\bar{V})$, msec

APPARATUS AND PROCEDURE

Some of the details of the test apparatus and procedures in this study are presented in this section. A more complete description of the drop tower and the experiment apparatus and procedures can be found in appendix A.

The diffusion flame together with a fuel flow system, a camera, and a clock were allowed to free-fall 23 meters within an air drag shield that maintained the gravity level below 10^{-5} (termed zero gravity in this report). The diffusion flame was ignited in normal gravity just before the beginning of the test. The flame burned on an upright circular cylindrical nozzle in quiescent air at standard temperature and pressure (fig. 1). The length of the nozzle was sufficient to assure that a fully developed parabolic velocity profile existed at the nozzle exit. Three fuels, ethylene, propylene, and hydrogen, were studied. Each fuel was used in conjunction with four nozzles with inside radii of 0.051, 0.083, 0.113, and 0.186 centimeter.

The ethylene and propylene flames were photographed with a high-speed (400 frames/sec), 16-millimeter camera using Ektachrome EF (tungsten) film. Depending on the flame size, pictures were taken with either a 17-, 25-, or a 35-millimeter lens with aperture settings of f 2.8, f 1.4, and f 1.1, respectively. The film was pro-

cessed to an ASA of 250.

Photographing the hydrogen flames presented a special problem. The light intensity emitted from such flames relative to hydrocarbon flames is almost negligible. Consequently, a 15-frame-per-second, 16-millimeter camera with Eastman Kodak high speed infrared film was used to photograph these hydrogen flames. Pictures were taken with a 35-millimeter lens using an aperture setting of f 1.1. A number 25 infrared Wratten filter was used over the camera lens. A few tests were made photographing low-flow-rate hydrogen flames using color as well as infrared film. The results of these tests indicated that the type of film used only nominally affects the photographed flame shape.

DATA REDUCTION

Flame length measurements as a function of time, as well as general observations, were made by viewing the motion picture film of the tests. The measurements were made with a motion picture film analyzer which enlarged the film image. The necessary measured length to actual length ratios (scale factors) were obtained by photographing a ruler with 0.1-centimeter divisions mounted above the nozzle for each lens that was used.

RESULTS AND DISCUSSION

Normal-Gravity Data

A series of calibration tests for each nozzle-fuel combination was run to establish the relations between axial flame length and flow rate for normal-gravity flames.

Observations. - Before the data are presented several observations are necessary in order to make these measurements more useful. As is typical of normal-gravity diffusion flames (ref. 6), the flames of all the test fuels appeared to flicker (vary in length) at the higher flow rates. The flickering amplitude was generally less than 30 percent of the average length. This average length was selected to be used for comparisons in this report. As the flow rate was increased for the ethylene and propylene fuels, the flame shape went from a flame front closed at the top (overventilated) to a flame with a finite width at its top (underventilated). For the underventilated flames observed with ethylene and propylene, the lengths were more difficult to measure since the flames appeared to gradually fade in color at their tops. The axial length chosen in this situation was the longest length at which any visible color was present. The hydrogen flames were always overventilated.

Quantitative data. - All of the normal-gravity axial flame length data were obtained from the calibration tests and are presented in figure 2. Although some scatter exists, the following trends may be seen in the data. For the flames of ethylene and propylene at the lower flow rates, the variation of average axial flame length with flow rate appears to be linear and independent of nozzle size. At the higher flow rates for these same fuels and for the entire flow rate range of the hydrogen fuel, the axial flame length became dependent on nozzle radius, and its variation with flow rate became nonlinear, particularly at the highest flow rates.

Edelman, Fortune, and Weilerstein (ref. 7) numerically solved the methane diffusion flame problem, with gravity effects included. Their results show a dependence of flame length on nozzle radius that corresponds to the experimental data shown herein. This dependence is attributed to the relative importance of buoyancy with changing nozzle size.

All of the maximum flame radius data for normal-gravity flames are presented in figure 3 and in table I. In general, the maximum flame radius increased as the flow was increased. Although there is some scatter in the data, it can also be seen that for a constant flow rate the maximum flame radius became larger as the nozzle radius was increased.

Correlations. - To correlate the normal-gravity data with the appropriate controlling parameters for all the fuels tested, it became necessary to evaluate the physical properties of the fuels. A summary of the pertinent fluid and combustion properties together with those of methane, which was used in a previous comparable study (ref. 5), are given in table II. All of the values used are available in handbooks except for the diffusion coefficients, which were calculated by using a mathematical model described in reference 9.

A correlation has been obtained for the normal-gravity maximum flame radius (fig. 4). The nondimensional maximum flame radius is shown to be a function of the fuel time τ_F, which is defined as the ratio of nozzle radius to average fuel velocity at the nozzle. The functional dependence was first analytically demonstrated for methane flames by Edelman, Fortune, and Weilerstein (ref. 7). Their result and the range of fuel times over which it was developed are shown in figure 4 as an unbroken line. The equation for this line is

$$\frac{R_{M1}}{R_0} = 5.75 - 3.70 \log \tau_F \tag{1}$$

This curve is in fair agreement with the methane data. It can be seen that, over the range of fuel times covered by this prediction, the same general trend is evident for all the present data. It should also be noted that the dimensionless maximum flame radius

ceases to be proportional the the logarithm of fuel time for fuel times greater than 5 milliseconds. In summary, a correlation between dimensionless normal-gravity maximum flame radius and fuel time has gathered the data of four radically different fuel gases over three orders of magnitude of the fuel time.

Zero-Gravity Data

A minimum of three flow rates were tested for each nozzle-fuel combination in zero gravity. For these tests the fuel was ignited in normal gravity, and several seconds were allocated to allow the flame to reach its normal-gravity configuration before the experiment began to free fall. (The test procedures are described in more detail in appendix A.)

Observations. - As was observed with other diffusion flames in zero gravity (ref. 5), within several hundredths of a second after entry into weightlessness, all of the flames underwent a sharp decrease in length. (Fig. 5 shows this occurrence in a typical plot of axial length with time.) They then began to change color and expand away from the nozzle. Finally, at the end of the drop the flames assumed one of two configurations: (1) they remained transient, or (2) they reached steady state.

It is of particular interest that none of the flames were extinguished on entry into weightlessness. This result is decidedly different than the results of Cochran (ref. 5) wherein a rather large domain of extinguished methane flames was observed. This result can be attributed to the fact that different fuels were used in the two studies. Transient flames (changing color and/or length throughout the test) were observed only for the fuel gases ethylene and propylene burning on 0.113-centimeter nozzles or larger. In all of the remaining tests a steady-state configuration was achieved within the 2.2 seconds of drop time.

It must be noted that none of the zero-gravity flames flickered. This result is in agreement with the findings of Cochran's zero-gravity methane flame experiments (ref. 5). It has been suggested (ref. 10) that flickering is caused by selective amplication of traveling Tollmien-Schlichting disturbance waves. The waves are amplified when the local Reynolds number in the flow exceeds some critical value. The absence of flickering in zero gravity may be explained by the lowering of the local Reynolds number through the flow field as a result of the absence of buoyancy.

The steady-state flames of the test fuels are shown in the photographs of figure 6. For comparison both the normal- and zero-gravity configurations for each test are given. The propylene and ethylene flames, as was seen in normal gravity, appeared to be either overventilated or underventilated depending on the flow rate. The particular flow rate at which the flame shape changed from the overventilated to the underventilated

condition seemed to be lower in zero gravity than in normal gravity. In contrast, the hydrogen flames were always overventilated in both normal and zero gravity. This behavior is similar to that observed by Cochran (ref. 5) for methane flames.

Another observation of flame behavior in zero gravity is shown in figure 6(e), which was obtained with infrared film. Independent of nozzle size or flow rate, the zero-gravity hydrogen flame appeared to be burning well below the top of the nozzle. Typically, the lowest point of the flame front was about 0.75 centimeter below the nozzle. This phenomena was not evident in normal gravity nor was it evident in any of the other tests conducted with the hydrocarbon fuels using color film. However, Cochran and Masica (ref. 3) photographed methane flames in zero gravity using infrared film and observed this same behavior. For the purposes of comparison and correlation the hydrogen zero-gravity length data do not include this added length, rather the length is a measurement of the distance from the top of the nozzle to the top of the flame.

The photographs of the steady-state hydrocarbon flames in zero gravity show that they have a distinctly different coloration than their counterparts in normal gravity. Typically, those flames in normal gravity have a bright yellow appearance over most of the flame with a pale blue region near the nozzle. In zero gravity the flames varied in color. At high flow rates the region near the flame tip tended toward a pale orange or red. The central part of the flame appeared bright yellow, and the region near the nozzle top was again pale orange or red. At low flow rates the entire flame was pale orange or red. In all of the transient hydrocarbon data, the color of the flame in zero gravity was a very pale red. All of the normal-gravity hydrogen flames, when observed in a darkened room, were a uniform pale pink over the entire flame. Because of the technique used to photograph zero-gravity hydrogen flames (black and white infrared film) a necessarily limited qualitative description of the flame can be given. When the flame entered weightlessness, it appeared to change from a relatively uniform light gray color to a uniform very light gray or white appearance. Because of the film and infrared filter used, this shift in tones of gray would indicate the light emitted from the hydrogen flame in zero gravity is shifted in wavelength further into the infrared. This occurrence is common to all of the test fuels. From radiation theory this would indicate cooler temperatures in at least parts of the reaction zone of the zero-gravity flames.

A final observation of flame appearance, seen in varying degrees in almost all of the hydrocarbon tests, concerned the sudden increase in soot or carbon particle production upon entry into weightlessness (see fig. 7). This sudden increase in soot production suggests a condition of partial oxidation (i.e., incomplete combustion) in parts of the reaction zone of the flame. Also, the increased soot production provides for many more sources of radiation losses and, therefore, could, in part, be responsible for the cooler hydrocarbon flame.

Quantitative data. - All of the steady-state normalized axial length data were plotted

as a function of the ambient fuel Reynolds number (fig. 8). The solid line on each graph represents the appropriate normal-gravity data from table I. As can be seen, the zero-gravity ethylene and hydrogen flames are longer than the normal-gravity flames at the same Reynolds number; the zero-gravity propylene flames are shorter. For comparison, methane flames in zero gravity are about 50 percent longer than their normal gravity counterparts (ref. 5).

The zero-gravity maximum flame radius data as a function of fuel flow rate is presented in figure 9. Upon examining figure 9 and comparing it with the normal-gravity radius data of figure 3, several trends become evident. Data for all the fuels indicate that the zero-gravity flames were larger than the width of the normal-gravity flames at a given flow rate. Cochran (ref. 5) found that the zero-gravity methane flame width was about $1\frac{1}{2}$ times the normal-gravity width. A second trend is seen when examining the zero-gravity data for a nozzle radius dependence. The zero-gravity data appears to be separated by nozzle radius much more distinctly than the normal gravity data as seen in figure 3.

Correlations. - To correlate the normalized flame length data for all the diffusion flames, a simplified analysis of the problem was performed by Haggard and Cochran (ref. 11), some details of which are found in appendix B.

As the result of the assumptions made in appendix B and the mathematical analysis described in reference 11, the zero gravity normalized flame length was found to be

$$\frac{L_s}{R_0} = 2\, S_c^{1/2}\, Re\, \ln^{1/2}\left(\frac{1}{1 - c_F}\right) \tag{2}$$

where Re is the Reynolds number (VR_0/ν), Sc is the Schmidt number (ν/D), and cF is the mole fraction of fuel at the reaction zone of the flame. The dependence of dimensionless axial length on Reynolds number was expected because of the experimental work of Cochran (ref. 5). It remained to more thoroughly examine the Reynolds number and Schmidt number dependence through fluid property variations and to test the natural logarithm parameter $\ln^{1/2}(1/1 - c_F)$ by burning fuel gases which have different limits of inflammability.

Subsequent experimental verification of this prediction was performed in reference 11 using only the hydrocarbon gases methane, ethylene, and propylene. The data were compared with theory by using the lower limit, the upper limit, and the stoichiometric burning mole fraction. The best fit to the data was given by

$$\frac{L_s}{R_0} = 3.5\, Sc^{1/2}\, Re\, \ln^{1/2}\left(\frac{1}{1 - c_S}\right) + 5 \tag{3}$$

where c_s is the fuel mole fraction for stoichiometric burning. The additive constant 5 is small and may be caused by scatter in the data. In figure 10 this correlation is graphically shown together with the hydrogen flame data. As can be seen from the figure the hydrogen data do not correlate with the hydrocarbon data. Instead, a best fit to the hydrogen data appears to be identically the theoretical solution (eq. (2)) with the flame zone fuel concentration equal to that concentration for stoichiometric burning.

The results presented in figure 10 show that for the same flow conditions, the hydrocarbon flame length is longer than the hydrogen length. This difference may be attributed to moving carbon particles (soot) radiating above the reaction zone of the hydrocarbon flame, increasing the apparent flame length. Because the carbon particles are very good radiators of heat, it may be expected that the hydrocarbon flame temperature will be reduced in zero gravity. This reduced temperature may also effect hydrocarbon flame length.

The dimensionless zero-gravity maximum flame radius is plotted as a function of fuel time τ_F in figure 11. The dashed line in the plot is the normal-gravity theoretical prediction from figure 4. The line through the zero-gravity data represents an extrapolation of the partial-gravity analytical work of Edelman, Fortune, and Weilerstein (ref. 7) who performed numerical calculations for methane flames at gravity levels from 0.1 to 1 and a separate analysis at zero gravity. Their zero-gravity numerical analysis did not correspond to the experimental flame width data, particularly at low Reynolds numbers. For gravity levels from 0.1 to 1, they found that the normalized maximum flame radius could be expressed as a function of gravity level in the form

$$\frac{R_M}{R_0} = 10.5\, e^{-0.603\bar{g}} - 3.7 \log \tau_F \qquad (4)$$

The solid line shown in figure 11 is a graphical representation of this equation with $\bar{g}$ set equal to zero. The experimental data presented in this report together with the work of Cochran (ref. 5) confirm both the validity of equation (4) at normal gravity (see fig. 4) as well as the validity of extrapolating equation (4) to zero gravity (see fig. 11).

Flame existence. - The flame conditions observed in zero gravity, as discussed in the preceding section, are displayed in figure 13 as functions of the ambient fuel Reynolds number (VR_0/ν) at the nozzle exit. The following trend is evident from the bar graphs (fig. 13): As the Reynolds number was increased, the flame conditions appeared in the order - extinguished, transient, steady-state overventilated, and steady-state underventilated.

The fact that transient effects were observed in the experiments is not surprising in view of the test technique. Further, their influence in defining the behavior of the flames is of considerable importance, particularly where the extinguished flames are

concerned. Edelman, Fortune, and Weilerstein (ref. 7) indicated that the extinguishment observed in drop tower testing is caused by these transient effects. Their explanation is that the transient fluid dynamics associated with the sudden removal of buoyancy results in an imbalance in the flames that promotes a reduction in temperature and an alteration in the chemical kinetics. For the steady-state flames that were observed, the characteristic time of the system was small enough to allow the flame to react fast enough to achieve a stable configuration. However, for the extinguished cases, the characteristic flow time was too long, and a cascading temperature resulted in extinguishment.

Certainly, the question of importance is not whether flames are extinguished or stable in drop tower tests but, in fact, what are the conditions under which flames can exist in a zero-gravity environment. The presence of transient fluid dynamics effects in the experiment raises the possibility that flames that were extinguished or that were transient could exist in a stable condition in zero gravity if the gas was ignited under the proper set of circumstances. However, the structure of flames that are known to be stable in zero-gravity indicates cool temperatures and the possibility of finite reaction rates distributed in space; inherent in these are high heat losses. This suggests that at relatively low flow rates where the extinguished and transient conditions prevail, the convective, radiative, and diffusive effects may not be sufficiently balanced to permit a reaction to be sustained.

SUMMARY OF RESULTS

An experimental investigation was performed on laminar hydrogen-, ethylene-, and propylene-air diffusion flames burning in a weightless environment. The flames burned on nozzles with radii ranging from 0.051 to 0.186 centimeter with fuel Reynolds numbers at the nozzle exit from 9 to 410. The results of this study are

1. The ratio of stable axial lengths L_s to nozzle radius R_0 for all hydrocarbon fuels in zero gravity is given by the relation

$$\frac{L_s}{R_0} = A\, Sc^{1/2}\, Re\, \ln^{1/2}\left(\frac{1}{1 - c_s}\right) + B$$

where Sc is the fuel Schmidt number, Re is the Reynolds number, c_s is the stoichiometric mole fraction, A is a constant equal to 3.5 for hydrocarbon flames and 2.0 for hydrogen flames, and B is a constant equal to 5.0 for hydrocarbon flames and 0 for hydrogen flames.

2. The ratio of maximum flame radius R_M to nozzle radius R_0 is given by the relation

$$\frac{R_M}{R_0} = 10.5\, e^{-0.603\bar{g}} - 3.7 \log\left(\frac{R_0}{\bar{V}}\right)$$

where $\bar{V}$ is the average flow velocity at the nozzle exit and $\bar{g}$ is the gravitational level. This result is in agreement with published analytical studies.

3. The hydrocarbon fuels studied produced transient flames (i.e., constantly changing length and color throughout the test) on nozzles with 0.113-centimeter radii or larger and steady-state flames on nozzles with radii 0.0825-centimeter or smaller in a weightless environment. All hydrogen flames were steady state in a weightless environment.

4. Heavier hydrocarbon flames dramatically increase soot production on entry into weightlessness. Flame coloration observations in a weightless environment indicate that parts of the flame are burning cooler. These observations suggest that the reaction zone may become thicker.

Lewis Research Center,
National Aeronautics and Space Administration,
Cleveland, Ohio, November 10, 1972,
502-28.

APPENDIX A

FURTHER DETAILS CONCERNING THE APPARATUS AND PROCEDURE

Test Facility

The experimental data for this study were obtained in the Lewis Research Center's 2.2-second zero-gravity facility. A schematic diagram of this facility is shown in figure 13. The facility consists of a building 6.4 meters (21 ft) square by 30.5 meters (100 ft) tall. Contained within the building is a drop area 27 meters (89 ft) long with a cross section of 1.5 by 2.75 meters (5 by 9 ft).

Mode of operation. - A 2.2-second period of weightlessness was obtained by allowing the experiment package to free fall from the top of the drop area. In order to minimize drag on the experiment package, it was enclosed in a drag shield, designed with a high ratio of weight to frontal area and low drag coefficient. The relative motion of the experiment package with respect to the drag shield during a test is shown in figure 14. Throughout the test the experiment package and drag shield fell freely and independently of each other; that is, no guide wires, electrical lines, and so forth were connected to either. Therefore, the only force acting on the freely falling experiment package was the air drag associated with the relative motion of the package within the enclosure of the drag shield. This air drag resulted in an equivalent gravitational acceleration acting on the experiment, which is estimated to be below 10^{-5} g's.

Release system. - The experiment package, installed within the drag shield was suspended at the top of the drop area by a highly stressed music wire that was attached to the release system. This release system consisted of a double-acting air cylinder with a hard steel knife attached to the piston. Pressurization of the air cylinder drove the knife edge against the wire, which was backed by anvil. The resulting notch caused the wire to fail, smoothly releasing the experiment. No measurable disturbances were imparted to the package by this release procedure.

Recovery system. - After the experiment package and drag shield traversed the total length of the drop tower, they were recovered after decelerating in a 2.2-meter (7-ft) deep container filled with sand. The deceleration rate (averaging 15 g's) was controlled by selectively varying the tips of the deceleration spikes mounted on the bottom of the drag shield (fig. 14). At the time of impact of the drag shield in the decelerator container, the experiment package had traversed the vertical distance within the drag shield (compare figs. 14(a) and (c)).

Experimental Package

The experimental package (fig. 15) contained a combustion chamber, camera, clock, fuel flow system, carbon dioxide flow system, and associated controls and direct-current power supplies.

The combustion chamber contained the nozzle, lighting equipment, carbon dioxide inlets, and the ignition system. The nozzle extended approximately 2 centimeters above the floor and was positioned at the center of the chamber. The dimensions of the chamber were approximately 41 centimeters long by 41 centimeters wide by 48 centimeters high. The top of the chamber had holes in it to ensure equalization of pressure with the atmosphere during burning. The volume of the chamber was such that there was over 60 times the amount of air necessary to burn the fuel at the highest flow rate for at least 10 seconds. The igniter was a coiled 0.33-centimeter-diameter Nichrome wire attached at its ends to copper rods. Current to the wire was supplied by a 14.4-volt, 1.75-ampere-hour pack of batteries. One wall of the chamber was a plastic sheet. Lighting was indirect so that the flames could be photographed against a black background.

The fuel flow system included a 500-cubic-centimeter stainless-steel vessel, flow valves, a relief valve, a low-flow needle valve, two explosion-proof solenoids, stainless-steel tubing, and a pressure regulator. In this system the solenoids were connected in series to ensure that flow stopped on deactivation.

Carbon dioxide was included to dilute the contents of the combustion chamber below the flammability limit after the test. This system consisted of two 500-cubic-centimeter stainless-steel vessels, flow valves, a relief valve, two explosion-proof solenoids, and stainless-steel tubing. Mounting of the solenoids in parallel ensured flow upon activation.

Test Procedure

Calibrations. - Before the normal- and zero-gravity experimentation, calibrations to determine flame length as a function of flow rate were conducted. The flow measuring device, a rotameter, was installed in the methane flow system. Motion pictures were then taken of flames at different lengths, and the respective flow rates were recorded. Data were obtained for each of the different nozzles over the range of flow to be used in the experiments.

Experimentation. - The fuel cylinder was charged to a pressure of approximately 14×10^5 newtons per square meter ($\sim$200 psi), and the carbon dioxide cylinders to about 34.5×10^5 newtons per square meter ($\sim$500 psi). The experiment package was placed in the drag shield and raised to the top of the tower.

Approximately 5 seconds before the drop, the lights were turned on, and the fuel flow, camera, and clock were started. One second later, the ignition system was activated. The remaining 4 seconds before the drop were used to permit the flame to come to steady state. The drag shield and experiment were released, and about 2 seconds of zero-gravity data were obtained. Just before impact in the sand, the fuel flow was stopped, the camera, clock, and lights were turned off, and the carbon dioxide system was activated. These steps removed potential ignition sources and diluted a possible combustible mixture.

APPENDIX B

ASSUMPTIONS USED IN ANALYSIS OF DIFFUSION FLAME AXIAL LENGTH

The basic geometry of the problem under consideration was given in figure 1. Pure hydrocarbon fuel gas in a fully developed parabolic velocity profile issues from a nozzle of radius R_0 and mixes with initially quiescent air at standard conditions in a weightless environment. A diffusion flame is defined as one in which the rate of mixing of fuel and oxidant, rather than the rate of chemical reaction, controls the process of combustion and in which burning takes place within an incandescent shell or reaction zone of axial length L. Under steady-state conditions the fuel and oxidant in the reaction zone must have concentrations that fall within the upper and lower limits of inflammability.

The following is a list of assumptions made in this analysis: (1) A stable laminar diffusion flame exists in zero gravity. (2) Fluid properties (i.e., density, dynamic viscosity, and diffusion coefficient) are constant within the volume enclosed by the reaction zone. This assumption was invoked in an effort to remove both concentration and temperature effects from the conservation of momentum and continuity equations. It is probably a most restrictive assumption near the reaction zone where the fuel is undergoing a sharp rise in temperature. (3) There exists no temperature or pressure driven diffusion (i.e., assume that Fick's law of diffusion holds). (4) The velocity profiles are such as to justify a similarity solution. This assumption does not appear valid for normal-gravity flames because of the gravity effects that accelerate the fluid, thus distorting the velocity profiles. However, this assumption should be valid in zero gravity sufficiently far enough downstream of the nozzle. (5) There is axisymmetric laminar flow throughout the flow field. (6) A boundary-layer type of flow exists where the axial velocity exhibits a strong radial dependence while dominating over the radial velocity.

REFERENCES

1. Andracchio, Charles R.; and Aydelott, John C.: Comparison of Flame Spreading Over Thin Flat Surfaces in Normal Gravity and Weightlessness in an Oxygen Environment. NASA TM X-1992, 1970.

2. Cochran, Thomas H.; Petrash, Donald A.; Andracchio, Charles R.; and Sotos, Ray G.: Burning of Teflon-Insulated Wires in Supercritical Oxygen at Normal and Zero Gravities. NASA TM X-2174, 1971.

3. Cochran, Thomas H.; and Masica, William J.: Effects of Gravity on Laminar Gas Jet Diffusion Flames. NASA TN D-5872, 1970.

4. Cochran, Thomas H.; and Masica, William J.: An Investigation of Gravity Effects on Laminar Gas-Jet Diffusion Flames. Thirteenth Symposium (International) on Combustion. Combustion Inst., 1970, pp. 821-829.

5. Cochran, Thomas H.: Experimental Investigation of Laminar Gas Jet Diffusion Flames in Zero Gravity. NASA TN D-6523, 1972.

6. Gaydon, Alfred G.; and Wolfhard, H. G.: Flames: Their Structure, Radiation, and Temperature. Third ed., Chapman and Hall, Ltd, 1970.

7. Edelman, R. B.; Fortune, O.; and Weilerstein, G.: Analytical Study of Gravity Effects on Laminar Diffusion Flames. Rep. GASL-TR-771, General Applied Science Labs., (NASA CR-120921), Feb. 1972.

8. Wohl, Kurt; Gazley, Carl; and Kapp, Numer M.: Diffusion Flames. Third Symposium on Combustion and Flame and Explosion Phenomena. Williams & Wilkens Co., 1949, pp. 288-300.

9. Reid, Robert C.; and Sherwood, T. K.: The Properties of Gases and Liquids: Their Estimation and Correlation. Second ed., McGraw-Hill Book Co., Inc., 1966.

10. Toong, Tau-Yi; Salant, Richard F.; Stopford, John M.; and Anderson, Griffin Y.: Mechanisms of Combustion Instability. Tenth Symposium (International) on Combustion. Combustion Inst., 1965, pp. 1301-1313.

11. Haggard, John B., Jr.; and Cochran, Thomas H.: Stable Hydrocarbon Diffusion Flames in a Weightless Environment. Combustion Sci. Tech., vol. 5, no. 6, Aug. 1972, pp. 291-298.

TABLE I. - SUMMARY OF EXPERIMENTAL FINDINGS

Run number	Nozzle radius, R_0, cm	Average normal-gravity length, L_1, cm	Maximum normal-gravity radius, R_{M1}, cm	Flow rate, Q, cm^3/sec	Steady-state zero-gravity length, L_S, cm	Zero-gravity maximum radius, R_{M0}, cm
			Ethylene			
1	0.051	8.63	0.39	3.55	10.40	0.54
2	↓	3.70	.31	1.62	5.25	.52
3		2.33	.32	1.07	3.90	.55
4		1.45	.29	.72	1.95	.54
5		.75	.19	.45	.90	.41
6	0.083	7.36	0.47	3.04	9.65	0.81
7	↓	4.48	.38	1.91	5.88	.81
8		3.03	.37	1.34	4.22	.83
9		2.16	.34	1.00	2.67	.71
10		1.19	.28	.62	1.49	.65
11	0.113	6.21	0.48	2.96	(a)	----
12	↓	4.80	.48	2.17	↓	----
13		2.88	.34	1.27		----
14		1.67	.26	.80		----
15		.80	.25	.46		----
16	0.186	5.45	0.52	2.74	(a)	----
17	↓	4.75	.40	2.10	↓	----
18		2.50	.36	1.12		----
19		.91	.24	.50		----
			Propylene			
20	0.051	11.68	0.40	2.87	9.58	0.65
21	↓	5.05	.29	1.24	3.61	.69
22		2.48	.26	.63	2.51	.74
23		1.78	.24	.47	1.79	.61
24	0.083	10.92	0.43	2.76	9.62	0.94
25	.083	4.81	.34	1.18	3.76	.84
26	.083	1.61	.28	.43	1.46	.67
27	0.113	8.33	0.57	2.30	(a)	----
28	↓	5.27	.33	1.28	↓	----
29		4.85	.34	1.20		----
30		3.46	.31	.84		----
31		2.64	.30	.64		----
32		1.24	.25	.29		----
33	0.186	9.13	0.59	3.38	(a)	----
34	↓	5.13	.37	1.21	↓	----
35		2.72	.33	.68		----
36		2.08	.31	.51		----
37		.74	.22	.23		----
			Hydrogen			
38	0.051	7.14	0.64	18.25	7.45	1.10
39	.051	5.00	.61	12.88	5.67	1.04
40	.051	2.40	.46	6.38	3.04	.76
41	0.083	7.61	1.03	20.60	8.67	1.56
42	.083	5.25	.79	14.53	5.69	1.25
43	.083	2.49	.46	7.40	3.12	.94
44	0.113	6.06	1.02	19.80	7.87	1.80
45	.113	4.35	.77	14.10	5.20	1.47
46	.113	2.22	.53	7.60	2.62	1.04
47	0.186	5.22	1.09	16.80	6.51	2.15
48	↓	4.35	.68	14.10	4.37	1.77
49		3.80	.72	12.25	4.67	1.78
50		1.81	.55	5.75	2.32	.73

[a]Transient flame condition.

TABLE II. - SUMMARY OF FUEL GAS FLUID AND COMBUSTION PROPERTIES[a]

Gas	Kinematic viscosity, ν, cm^2/sec	Calculated diffusion coefficient fuel into air, D, cm^2/sec	Schmidt number Sc, ν/D	Fuel mole fraction in air at limits of flammability		Fuel mole fraction for stoichiometric burning, c_s
				Lower limit, c_L	Upper limit, c_U	
Methane	0.1648	0.213	0.774	0.053	0.15	0.095
Ethylene	.0858	.152	.565	.031	.32	.065
Propylene	.0437	.117	.374	.024	.103	.0445
Hydrogen	1.059	.689	1.53	.04	.75	.295

[a]Properties given at 20° C and 1 A.

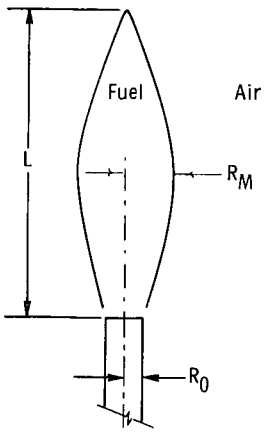

Figure 1. - Geometry of a diffusion flame on a nozzle.

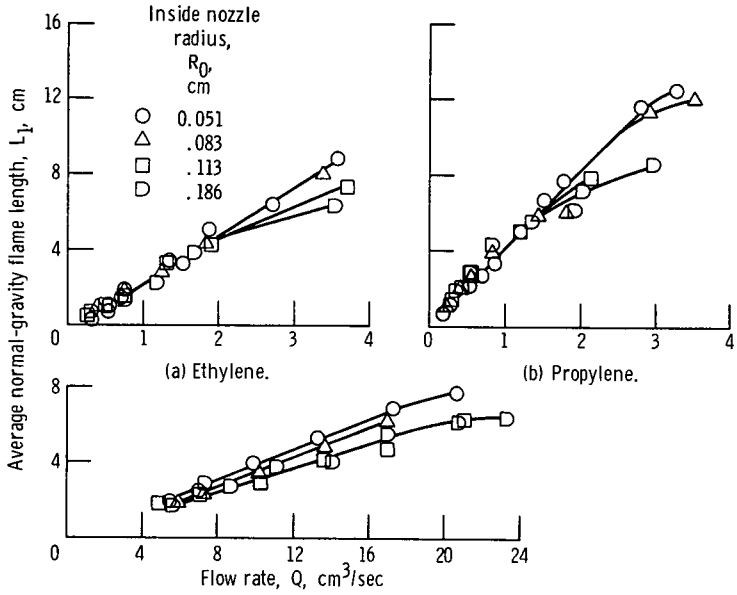

(c) Hydrogen.

Figure 2. - Average normal-gravity flame lengths of test fuels.

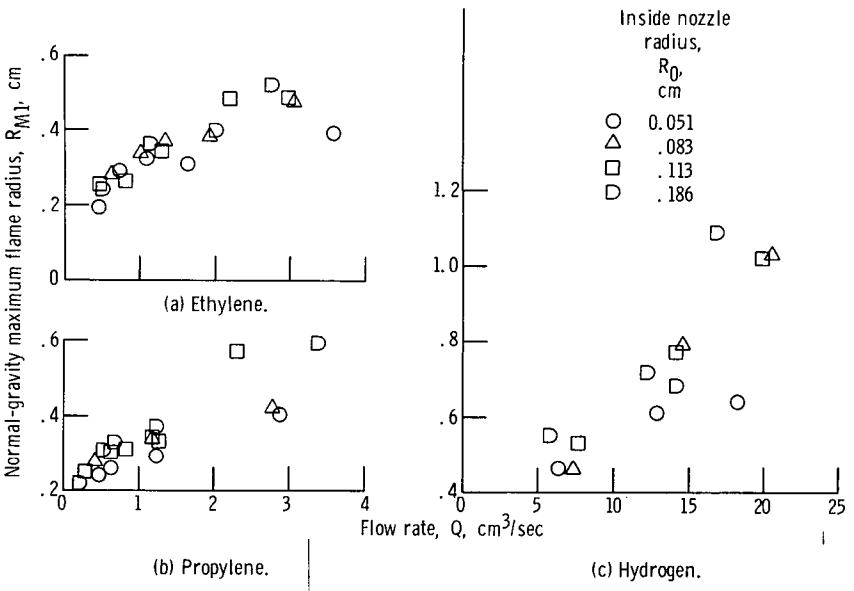

Figure 3. - Normal-gravity maximum flame radius of test fuels.

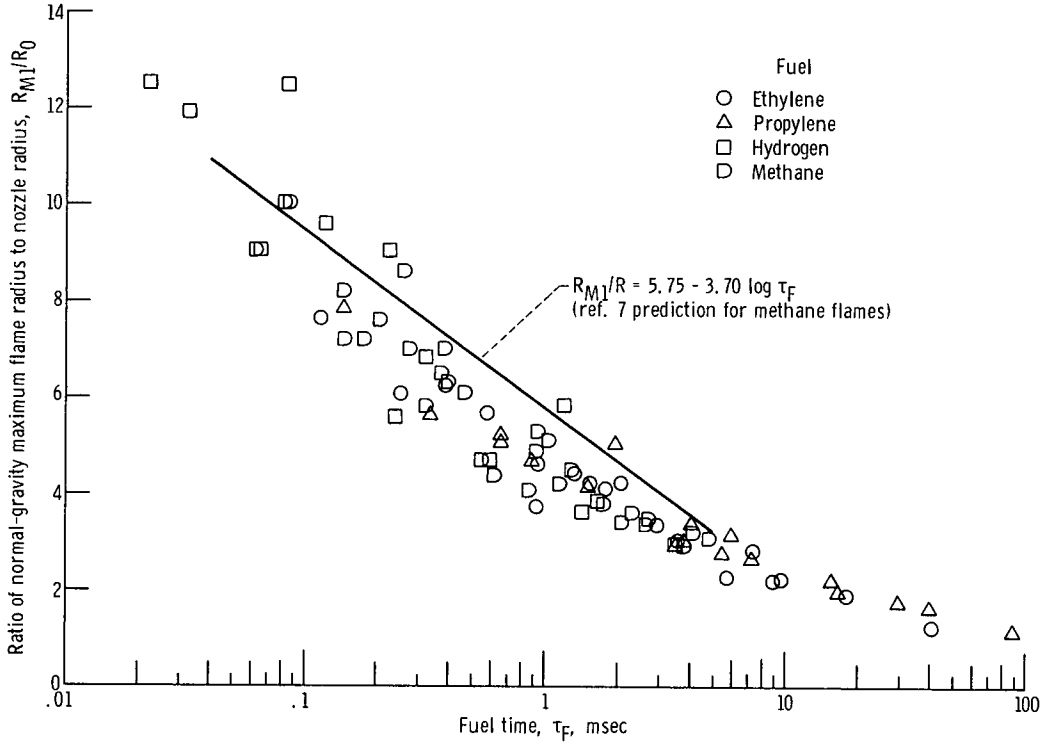

Figure 4. - Correlation of normalized flame radius with fuel time for normal-gravity flames.

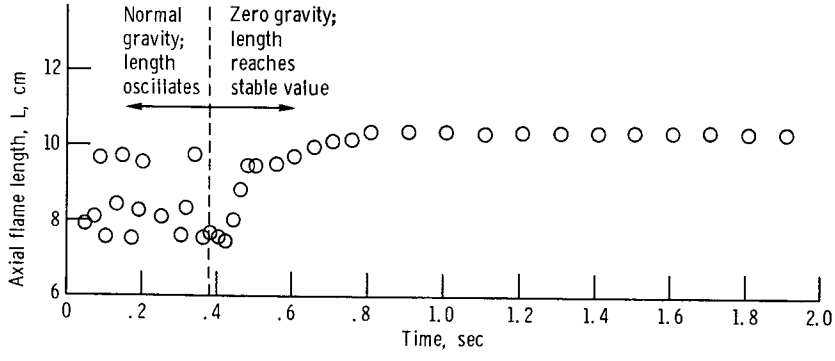

Figure 5. - Typical time profile of axial flame length upon entry into weightlessness. Run 1.

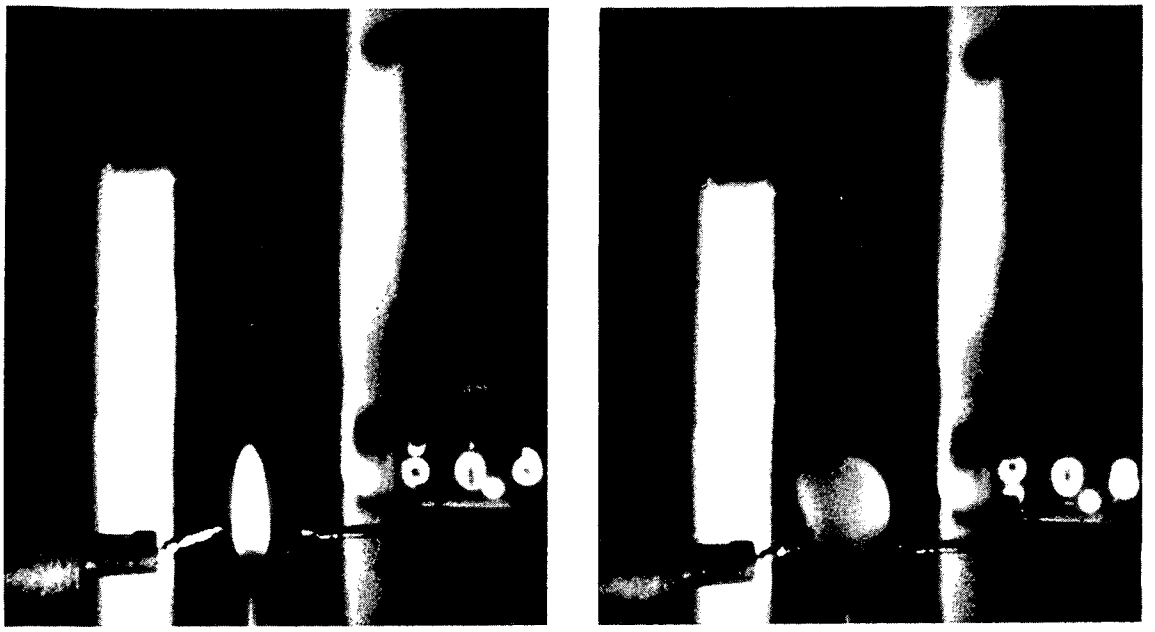

Normal gravity Zero gravity

(a) Overventilated propylene flame run No. 23.

Normal gravity Zero gravity

(b) Underventilated propylene flame run No. 22.

Figure 6. - Stable diffusion flames in weightlessness.

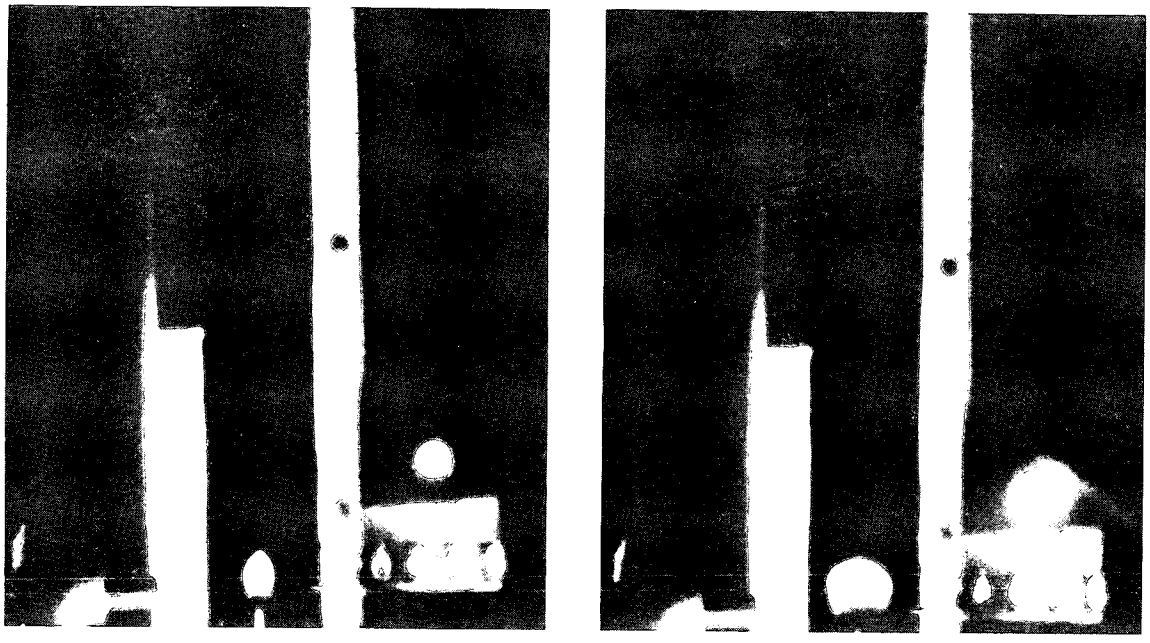

Normal gravity Zero gravity

(c) Overventilated ethylene flame run No. 10.

Normal gravity Zero gravity

(d) Underventilated ethylene flame run No. 7.

Figure 6. - Continued.

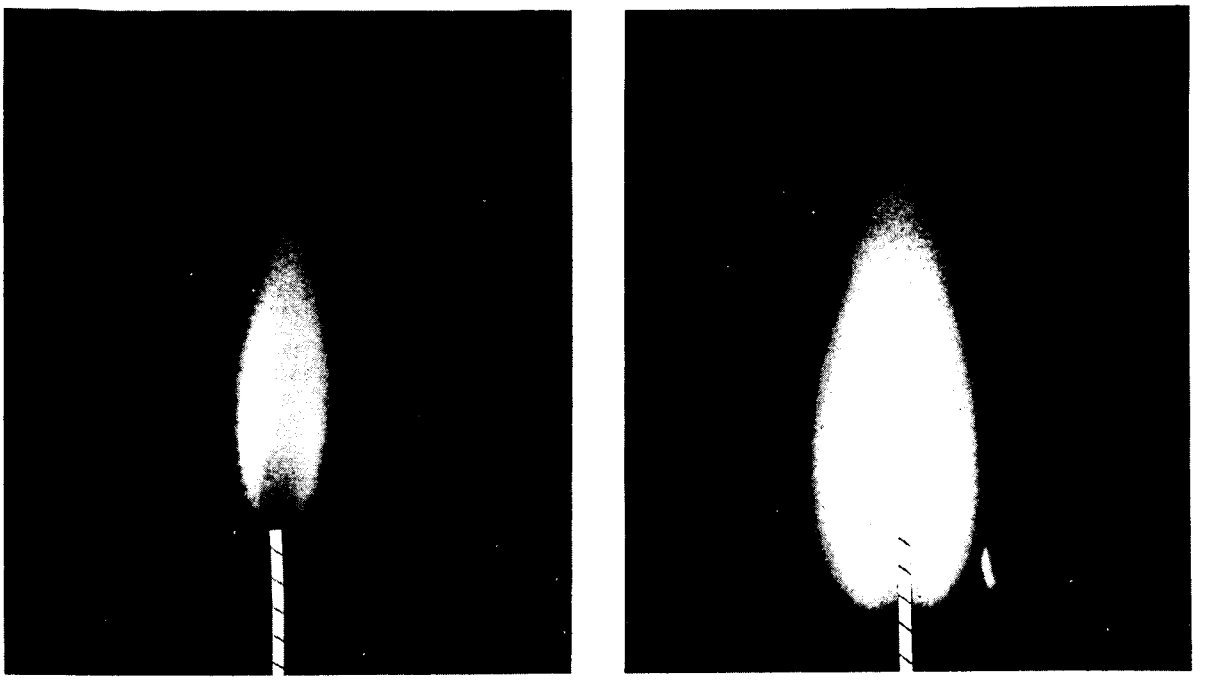

Normal gravity

Zero gravity

(e) Hydrogen flame run No. 39.

Figure 6. Concluded.

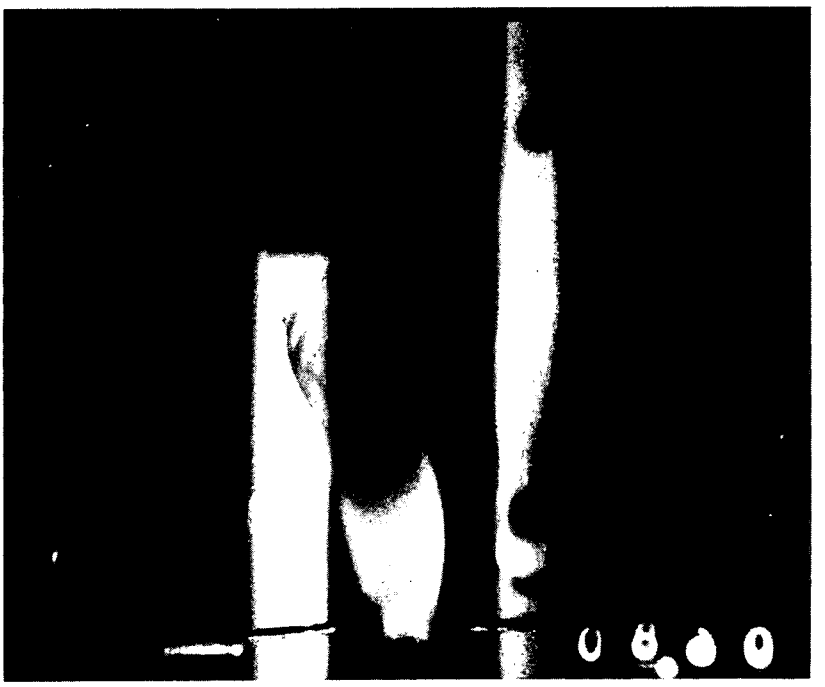

Figure 7. - A typical hydrocarbon flame producing large quantities of soot in zero-gravity. Zero-gravity propylene flame run No. 23.

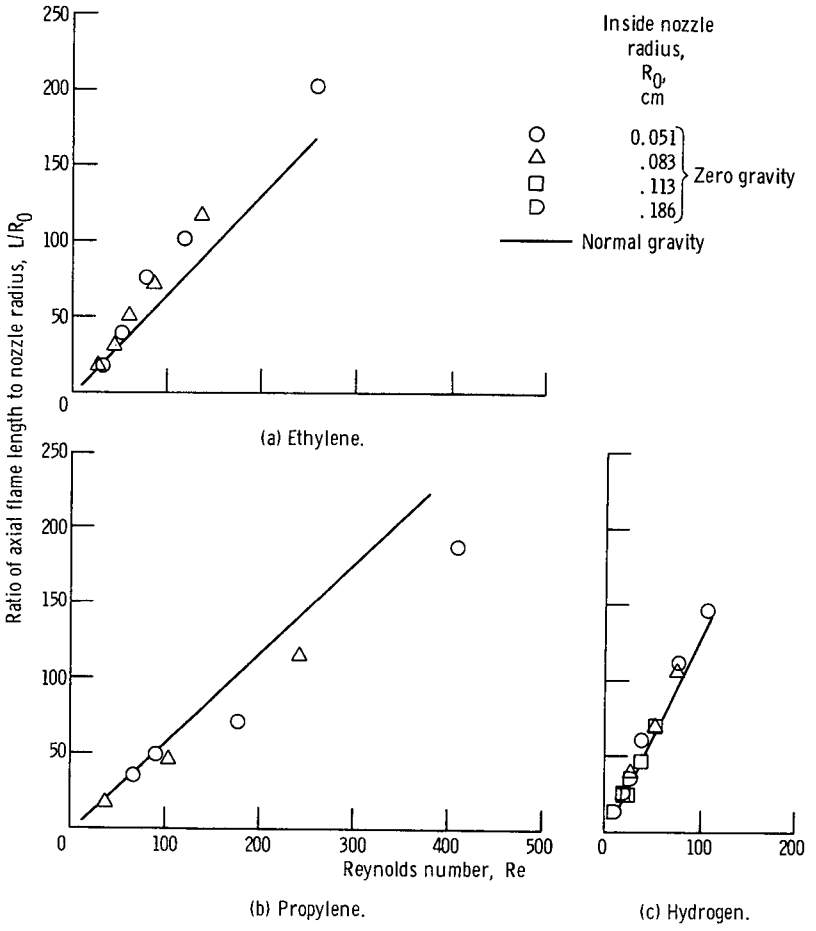

Figure 8. - Dimensionless axial flame length as function of Reynolds number for zero-gravity flames.

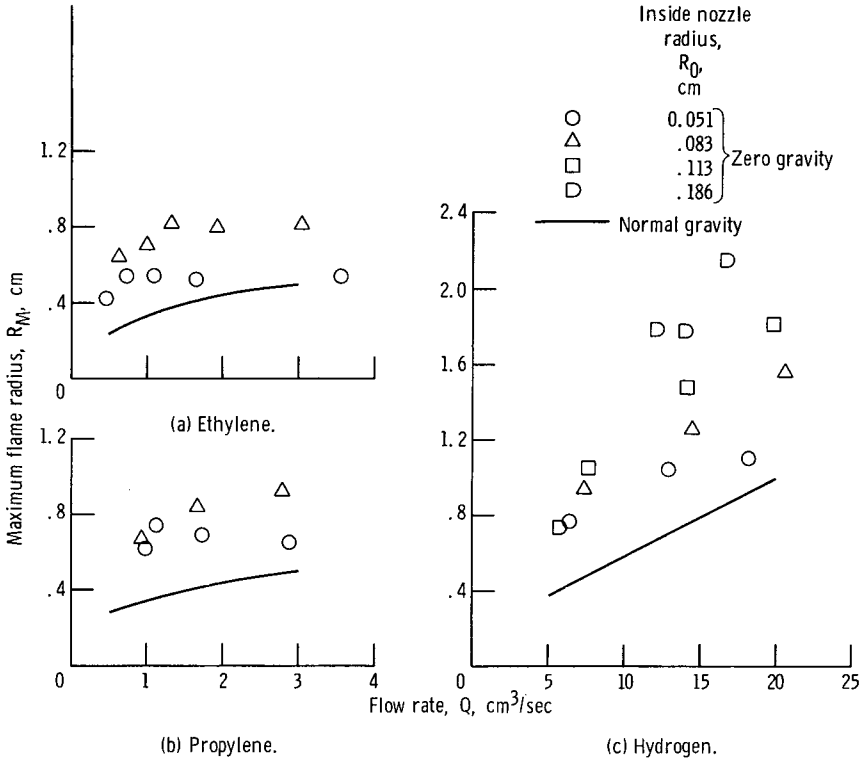

Figure 9. - Zero-gravity maximum flame radius of test fuels.

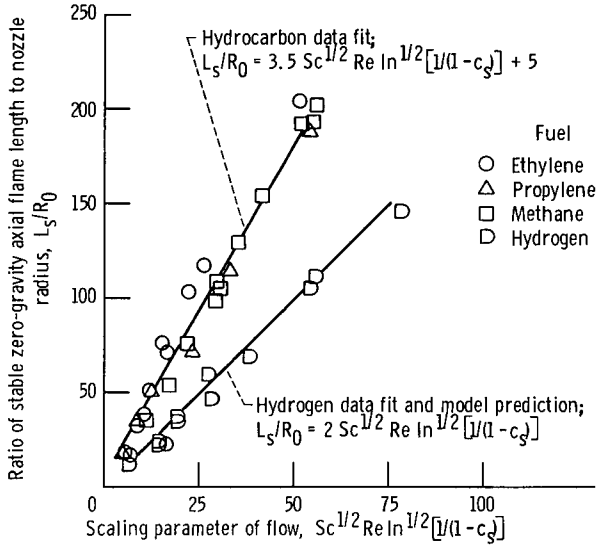

Figure 10. - Summary plot showing best fit of zero-gravity length correlation to data.

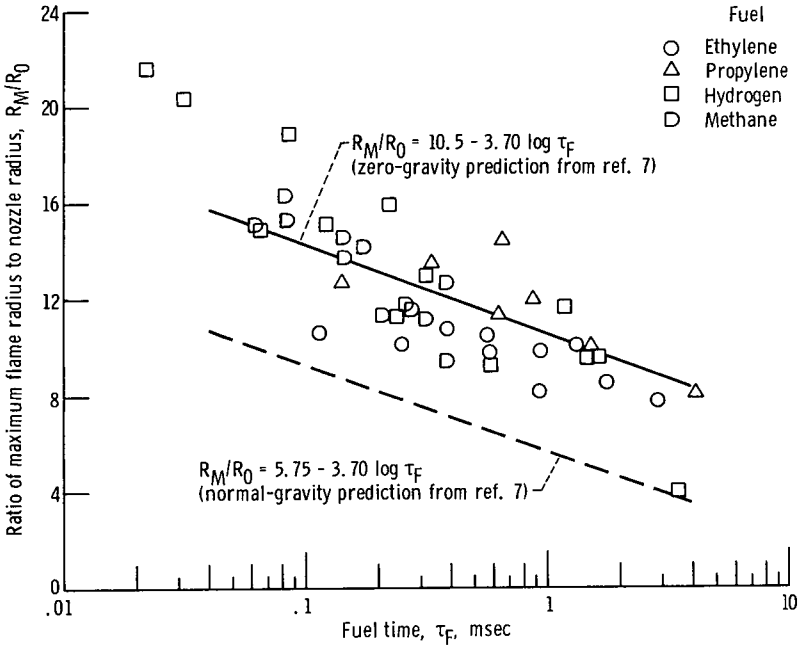

Figure 11. - Correlation of normalized maximum flame radius with fuel time for zero-gravity flames.

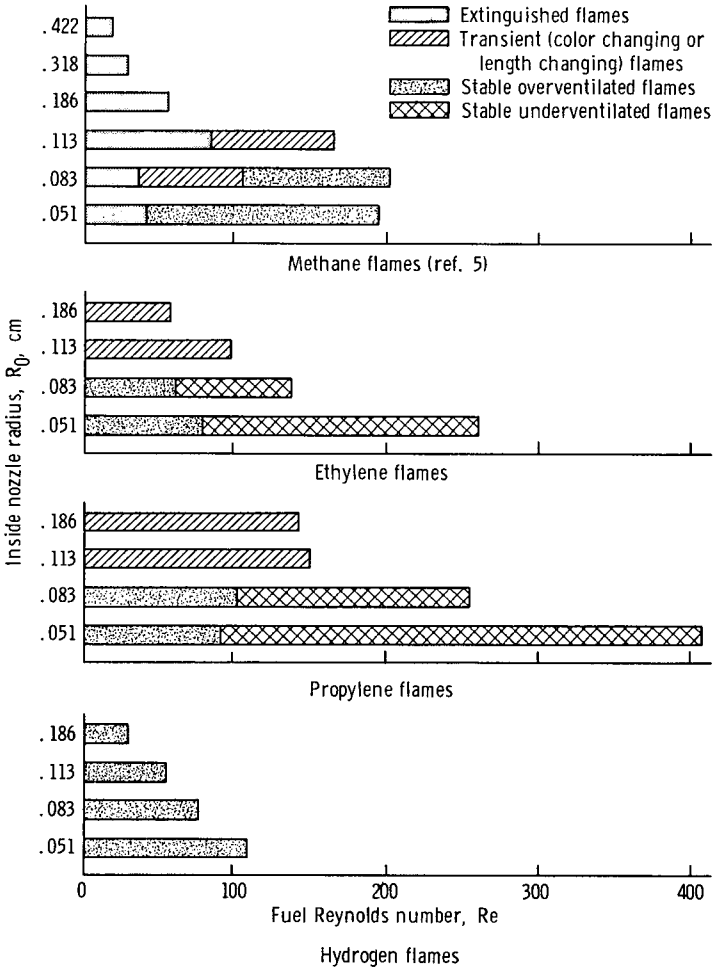

Figure 12. - Flame conditions encountered in zero gravity as function of flow.

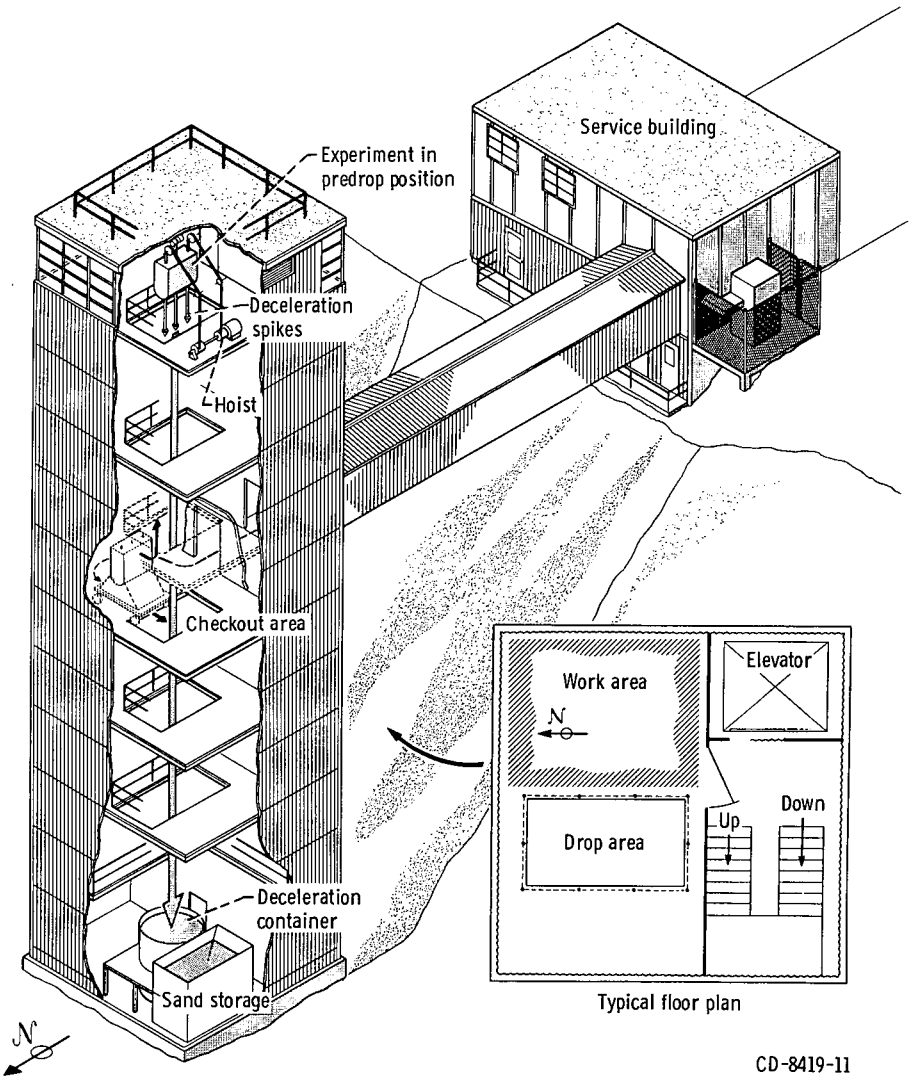

Figure 13. - 2.2-Second zero-gravity facility.

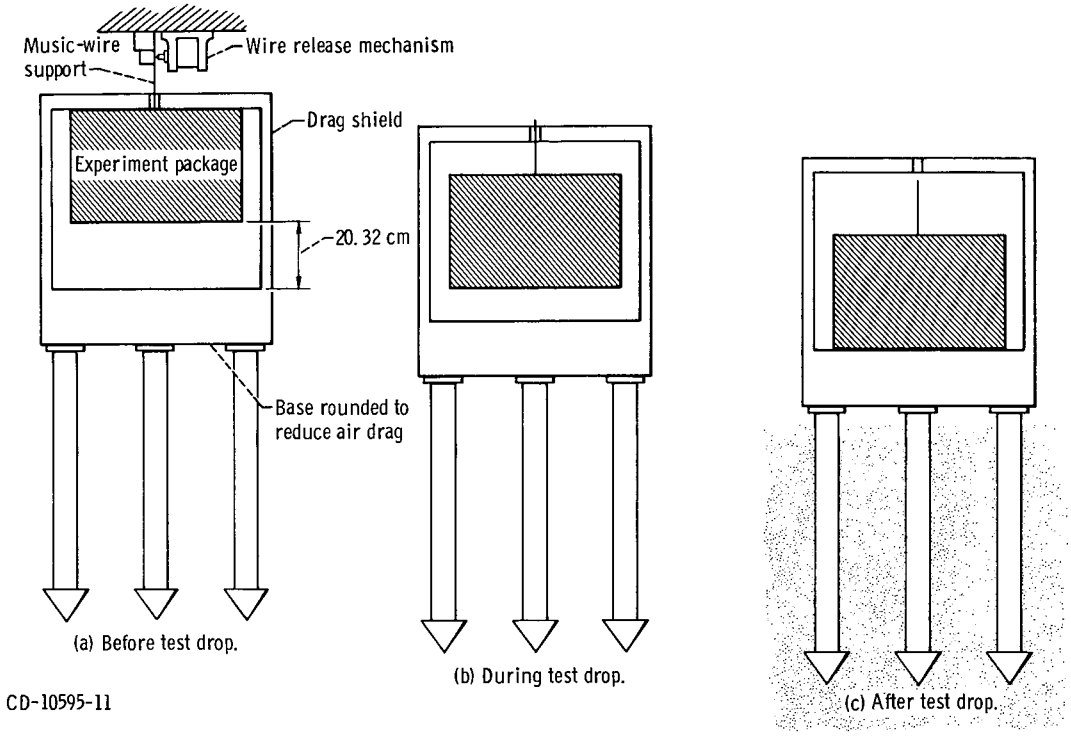

Figure 14. - Position of experiment package and drag shield before, during, and after test drop.

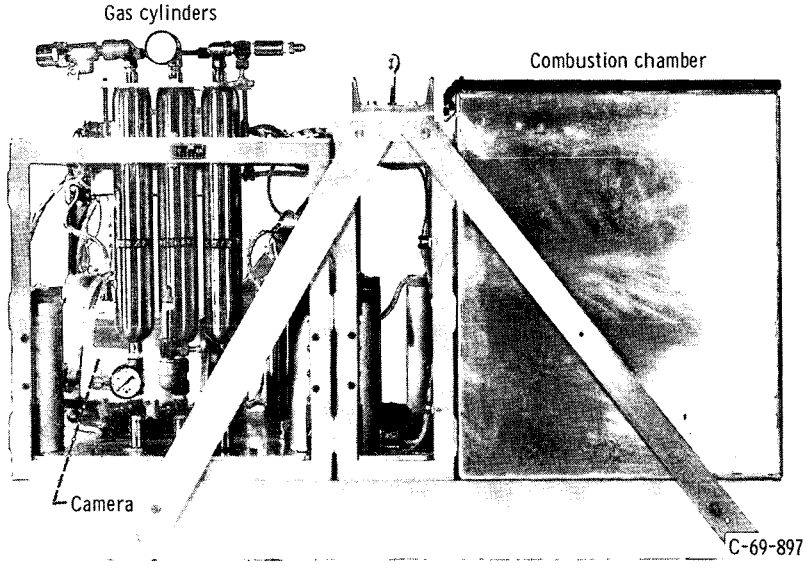

Figure 15. - Experiment package.

NASA-Langley, 1973 —— 33 E-6687